**Perception ms. 5691 TT**

# The effects of curvature on the grid illusions

Michael W. Levine

J. Jason McAnany

Department of Psychology and Laboratory for Integrative Neuroscience

University of Illinois at Chicago, Chicago, IL

Address for Correspondence:

Dr. Michael Levine
Department of Psychology, m/c 285
1007 West Harrison Street
Chicago, IL 60607-7137

Ph: 312-996-6133
Fax: 312-413-4122
Email: mikel@uic.edu

Running title: Curved alleys

Key words: Illusions, vanishing disk, scintillating grid, distorted grids

**Abstract.** Grid illusions, including the Hermann grid and scintillating grid (in which light disks are superimposed upon the grid intersections), are diminished by curving the alleys that limn the repeating pattern. Curvature might either disrupt the processes that induce the illusion, or simply make the illusory effects harder to see. To determine which mechanism might be invoked, we examined the effects of curving the alleys upon the vanishing disk illusion, a phenomenon in which a single disk in a grid intersection is rendered less detectable. This illusion is of reduced visibility, rather than generating an illusory apparition as in the Hermann grid or scintillating grid. Thus, inhibition of illusory influence would enhance disk visibility, while a general reduction of visibility would render disks even harder to detect. We find that thresholds for both scintillation and the disk itself increase in a graded manner with increased curvature. Measuring the effect of curvature upon the vanishing disk with traditional forced-choice staircase methods demonstrates that the effect of curvature is upon detection, not subjective criterion. Furthermore, disks that are easy to detect within a rectilinear grid are more difficult to detect when the alleys are curved. Thus, curvature of the alleys induces a general tendency to inhibit the visibility of features, and is not specifically a repression of illusory effects.

## 1 Introduction

Several visual illusions depend upon an array of boxes separated by a grid of narrow alleys. The best known of these is the Hermann grid, in which gray “smudges” appear at the intersections of the white alleys that define the solid black boxes. The textbook explanation for this effect is that there is more lateral inhibition upon cells in the intersections, being inhibited from four alleys, than upon cells within an alley, where there is inhibition from only two directions.

A feature of this illusion is that the smudges typically do not appear at the intersection being fixated; one explanation for this is that the macular receptive fields are so small that even their surrounds lie entirely within an alley or an intersection. Indeed, very small grids can show smudges in the fixated intersection; therefore the Hermann grid illusion has been invoked as a tool to measure “perceptive fields” (Spillmann 1994; Ehrenstein et al 2003). This is consistent with a lateral inhibition explanation of the illusion.

To quantify these effects, Schrauf et al (1997) attempted to cancel the smudges with disks more luminous than the alleys. They found a new effect: disks much brighter than the alleys displayed a transient sharp, black central spot. These spots appeared and vanished as the display was freely viewed, leading to the name “scintillating grid” for this illusion.

In our attempts to examine the origin of these illusions, we prepared a reduced scintillating grid with a single light disk, and noticed yet another effect: the disk vanished when the grid was fixated at a point well above or well below the disk (McAnany and Levine 2004). The disk was undetectable during fixation, or when the entire display was flashed for periods too brief to allow for saccades; dark disks, on the other hand, were relatively easily seen.

A demonstration of these effects is presented in figure 1. The left half of the figure contains a traditional rectilinear grid. Fixate on the cross at the bottom, and the white disk in the left intersection may vanish. This is not simply an effect of the inability of peripheral vision to resolve the disk, for the lower contrast disk slightly displaced from the middle intersection and the dark disk in the right intersection remain visible. With free eye movements, the white disk may scintillate. The strength of these effects depends upon eccentricity, so fixation above or below the cross may be necessary to appreciate the effects.

figure 1 near here

Geier et al (2004) produced grids in which the alleys wended a sinusoidal course between intersections. When the alleys were curved in this way, subjects reported that both the Hermann grid smudges and scintillating grid scintillations failed to appear (right half of figure 1; Schiller and Carvey 2005). This was interpreted as indicating that these effects are not due to lateral inhibition, since the net inhibition at intersections is identical for both straight and curved alleys.

We now ask whether curving the alleys would have a similar effect upon the vanishing disk, as a diagnostic for the effects of curvature. The Hermann grid and scintillating grid are both illusions in which a percept is generated of a feature not in the stimulus; the vanishing disk is an illusion in which a physical feature is rendered invisible. If curvature affects illusory processes, a disk that would vanish should no longer be obscured when the alleys are curved; if it affects visibility, the vanishing disk should vanish even more effectively.

## 2 Methods

### 2.1 *Subjects and stimuli*

The authors served as the principal subjects for these experiments. We were the only subjects for pilot work and a series of explorations of the possible effects of varying the parameters of the display. In addition, two naïve subjects (one male and one female) were tested for at least one run of each condition. A fifth subject graduated after completing only one run; his data were consistent with the other subjects, but were not included in the analyses. The procedures were approved by the University of Illinois at Chicago Institutional Review Board.

Stimuli were presented on an EIZO 19” FlexScan FX-D7 display monitor (1024 X 768 pixels, 85 Hz refresh rate) placed 35 cm in front of the subject. This distance is about the short end of reading or computer viewing distance. No subject noted discomfort at this viewing distance. The subject’s head was stabilized on chin and forehead rests. The monitor supplied the only significant light in the room. The screen was set to a neutral gray before and after each stimulus presentation; the same gray was used for the alleys and screen background. The gray chosen was about 18 cd/m$^2$, but different luminances were used for different series of runs in order to provide a range over which each subject could attain threshold for different degrees of curvature of the alleys within that series. These luminances ranged from 7.7 to 26.7 cd/m$^2$. The dark tetragons (which are not straight-edged when the alleys are curved) had a luminance of 0.19 cd/m$^2$, the darkest the monitor produced. The maximum available disk luminance was 51.29 cd/m$^2$.

The display consisted of two blocks of tetragons, one block above fixation and one below. The extent of the blank area between these blocks could be varied to establish the eccentricity of the stimuli. Greater separation (more eccentric stimuli) reduced visibility so the disks might not be visible even at the highest luminance available; closer separation made the task so easy that differences fell within the resolution of the gray scale. The maximum separation available placed the disks 13$^o$ above and below fixation; the minimum placed them 5$^o$ above and below. Various combinations of alley luminance and separations were used to test for the sensitivity of the effects to these parameters; these variations were used for subjects 1 and 2, so their data include many runs with various parameters. These parameters affected overall thresholds, but did not have a qualitative effect upon the role of curvature in changing thresholds. Although the specific parameter set varied among subjects, each subject was tested with the same parameter set in at least one run of each of the experimental conditions as in the other conditions. Each run comprising a series of curvatures was made with all other parameters held constant.

Each block consisted of two rows of four tetragons, thus defining three intersections. The alleys were 0.46$^o$ wide. As shown in figure 2, disks could be placed in the extreme intersections, which were 4.7$^o$ left or right of the vertical centerline. The radius of the disks was 0.29$^o$ in most runs; smaller disks (0.21$^o$) were used in some later runs (see Experiment 2), so that when disks were positioned along the alleys such that they were not centered within the intersections ("out of intersections") they would not partially eclipse the tetragons.

figure 2 near here

Alleys were curved according to a sine wave with a period matched to the spacing of the tetragons. Curvature, expressed by the amplitude of the sine as a percentage of its period, generally ranged from 0% (straight alleys) to 7.1%. At 7.1%, a tangent to the alley as it departs the intersection is at an angle of 22.6$^o$, and a line from the center of the intersection to the middle of the alley at its peak is at 15.9$^o$. The alleys in a given display all joined the intersections at the same angles, appearing as a clockwise twist (as in figure 2).

Stimuli were presented for 280 ms. Following each stimulus presentation the stimulus was replaced by a gray response screen of the same luminance as the previous background. The response screen had four large black outline squares, one in each quadrant of the screen, plus a red outline circle in the middle of the screen. The subject clicked on the quadrant that contained the target stimulus. A click in the red circle indicated failure to detect the target.

2.2 *Psychophysical methods*

A staircase procedure was used to determine thresholds for scintillation or visibility of the disks. Since scintillation is a phenomenon that is present when disks are clearly visible, we could not use a traditional forced choice in which only one disk was presented. The subject would know which intersection should have scintillation if it were the only intersection containing a disk. It was thus necessary to present a disk in all of the possible locations, but it would not then be possible to control which one should scintillate unless it were of a higher luminance, and the subject could then respond according to luminance.

We therefore devised a paradigm in which disks were present in all four of the possible locations, but asked the subject to select the disk with the most salient scintillation. If no scintillation was observed, the subject was instructed to select the red circle in the center of the response screen.

Whichever disk was selected was then decreased in luminance by eight units. The three disks not selected were each increased by a step of one unit. Thus, the chosen disk would decrease in luminance so that it should no longer be as effective, while the others increased in luminance and so could become more potent. When no disk seemed to scintillate and the red circle was selected, all four disks increased in luminance by two units so that they would become more effective. Note that the step sizes were limited by the 8-bit resolution of the video card, but the gamma function was nearly linear in the range about which the staircases converged.

The red circle default (indicating failure to detect) was necessary for the staircases to achieve stable asymptotes. The decrement step had to be sufficiently greater than the increments to allow the mean luminance of the four disks to descend to the threshold level; if it were exactly thrice the increment, the mean would remain the same after every trial. If it were less than thrice, the mean would increase until all disks were at maximum luminance. But with greater decrements, all the disks would converge upon zero contrast*. The choice that none were visible prevents this outcome, and the staircases efficiently converge to a threshold value.

The staircases proceeded until the luminances of each of the four disks vacillated about a stable level for at least 20 trials. The mean luminances of each disk over the final 20 trials was taken as its threshold. Since the threshold differences among disks were generally inconsistent, the four thresholds were averaged to represent mean threshold for that amplitude of curvature. We refer to this paradigm as the "simultaneous staircase method." The same technique was used to examine the vanishing disk; there, the subject's task was to indicate which disk (if any) was most clearly visible.

A subjective method is necessary to examine scintillation, but this leaves open the possibility that only the reporting of scintillation (or visibility) is affected by curvature, not its detectability. To verify that curvature affected detection, we used traditional forced choice staircase methods for the detection of the disks.

The simplest test was to interlace four independent traditional staircases, one for each possible position of the disk. The disk appeared at random in one of the four positions; the subject made a four alternative forced choice decision as to which position it was in ("nothing visible" was not allowed). The decision only affected the disk actually presented. Two correct responses in a row, disregarding trials in which the disk was in other positions, resulted in a decrease in luminance of that disk on its next presentation in that position; an incorrect response increased luminance by twice as much as the decrement step. We refer to this paradigm as "four separate interlaced staircases."

A potential drawback to the four separate interlaced staircases method is that if a subject strongly favored a particular location (and selected it whenever unsure), that location would enjoy more correct responses and show a low threshold at the expense of the other locations. While we never observed this occurring, we countered the possibility with another interlaced method. This paradigm appeared identical to the four separate staircases (a 4AFC task), but the two upper disks changed luminance in tandem, and the two lower disks changed in tandem. Thus, if the subject was biased to select a particular location when unsure, that staircase would rise when the other location was offered and indicate a high threshold. We refer to this paradigm as "two separate interlaced staircases."

The interlaced staircases proceeded until there were at least 12 reversals of each staircase; they continued beyond that if the experimenter judged that stable plateaus had not been attained despite the reversals. Threshold of each was taken as the mean luminance of the last six reversals. Since the threshold differences among disks at different positions were generally inconsistent, the thresholds were averaged to represent threshold luminance for that amplitude of curvature.

2.3 *Statistical methods*

Thresholds were taken as the Weber contrast of the mean threshold luminances. Data from each run were plotted as contrast thresholds *versus* curvature.

The relationship between threshold and curvature for each run was quantified by the Pearson correlation coefficient. A positive correlation implies that the threshold increases with curvature. To achieve a strong correlation, the data must be relatively consistent and increase in a reasonably linear progression. Thus, if an effect switched on in an all-or-none fashion, the correlation would be positive but small. In the occasional run in which the subject was unable to detect the disk at the maximum contrast available, only the point at the lowest curvature that reached the ceiling was included in the correlation. The data from any run were included only if there were at least three curvatures at which threshold was realized.

For statistical tests and estimating error ranges, correlations are not satisfactory because they are not normally distributed. Therefore, a normalizing transform, the Fisher *z* transform, was applied to the Pearson coefficients. All statistics, including means, *t*-tests for a difference from zero, and 95% confidence intervals, were performed on the transformed correlations. For presentation, the means and error ranges were translated back into the familiar correlation coefficients by the inverse Fisher *z* transform.

## 3 Experiments and Results

### 3.1 *Experiment 1: Effect of curvature on scintillation and the vanishing disk*

We first wanted to verify the effect of curvature upon scintillation, and test for the vanishing disk under comparable conditions and with the same paradigm. We further wished to determine whether the effect of curvature was an all-or-none phenomenon that was manifest at some minimum curvature, or was graded so that the effect was greater at larger curvatures.

For all subjects tested, it was clear that even minimal curvature had an effect upon scintillation. Averaged results from each of the four subjects are shown in figure 3A. For ease of comparison among subjects, contrasts are expressed as the fraction of the maximum contrast available, given the luminance of the alleys. Even relatively slight curvature increased thresholds, but thresholds continued to increase with greater curvature.

figure 3 near here

The mean correlations for each subject and for the combined data from all subjects are shown in figure 4 (left set of bars). The mean correlations (taken as the inverse transform of the mean Fisher *z* transforms of the correlations between the mean contrast thresholds and curvature of each separate run) were all quite high, and were significantly greater than zero for each of the two individuals who completed three or more such runs. The inverse transformed mean of all four subjects was 0.89; this value was also significantly greater than zero ($t$ = 8.820, 21 *df*, $p \ll 0.001$). The high positive correlation indicates that not only did threshold for scintillation increase with greater curvature, the increase was not an abrupt all-or-nothing step. This was also evident from the individual curves.

figure 4 near here

A similar result was obtained for threshold of the disk (the vanishing disk illusion). Data from all four subjects are shown figure 3B, with the inverse transforms of the mean transform of correlations in the middle part of figure 4. The correlations were again high; the inverse transformed mean of all four subjects was 0.76, and each of the four subjects had correlations significantly greater than zero ($p$<0.05). The mean for all subjects was highly significant ($t$ = 7.064, 56 *df*, $p \ll$ 0.001). The somewhat lower correlations may have been due to some irregularity at low curvature, which will be considered in the DISCUSSION. These effects may be appreciated from the left disks in figure 1. Compare the appearance of the disks in the right half of the figure with that of those in the left half.

Since thresholds obtained with the simultaneous staircase method depend upon the subject's criterion for when to select "nothing visible", thresholds were also measured with standard 4AFC staircases. For each of the three subjects tested with four interlaced staircases, and the four subjects tested with two interlaced staircases (upper and lower visual fields), the functions obtained by these methods were comparable to the corresponding functions obtained from that subject with the simultaneous staircase method using the same parameters. The only noticeable difference was that thresholds were slightly lower with the pure forced choice interlaced staircases, as might be expected when criterion is not a factor. The correlations between threshold and curvature obtained with these methods are shown in the smaller graphs on the right side of figure 4. The inverse transformed mean correlation across the three subjects tested with four interlaced stairs (upper graph) was 0.80 ($t = 9.284$, 4 *df*, $p < 0.001$). The inverse transformed mean correlation across the four subjects tested with two interlaced stairs (lower graph) was 0.73 ($t = 4.036$, 12 *df*, $p < 0.002$). These correlations straddle those derived from the simultaneous staircase method. The rise in threshold with curvature cannot be attributed to an alteration of the subject's criterion.

### 3.2 *Experiment 2: Visibility when the vanishing disk illusion is not evident*

The results of the first experiment show that the vanishing disk effect is stronger when the alleys are curved. We now ask whether this is specific to the illusory effects associated with the grid illusions (Hermann grid, scintillating grid, and vanishing disk), or is a more general effect. To test this, we explored the effects of curvature upon stimuli that do not vanish within grids.

Previous work has shown that only disks lighter than the alleys vanish effectively in the presence of black boxes (McAnany and Levine 2004). When the disk is also darker than the alleys, it remains visible (again see figure 1). The threshold contrast for dark disks is dramatically less in absolute contrast than that for light disks, although not as low as for disks in the absence of a grid. We had previously attributed the elevated threshold of dark disks in the presence of boxes (compared to no boxes) to the effective loss of contrast due to the lower mean luminance when dark boxes were present (McAnany and Levine 2004).

Increased curvature of alleys also rendered dark disks less visible, as evidenced by an increase in the absolute contrast required for threshold. Results for the four subjects are shown in figure 5A. It is clear that curvature produces an increase in threshold. The inverse transform of the mean transformed correlations from the four subjects tested was 0.97; the difference from zero was significant ($t$=18.805, 7 *df*, $p \ll 0.001$) (left side of figure 5B).

figure 5 near here

Another feature of the vanishing disk illusion is that the disk must be centered within an intersection if it is to vanish. As may be seen in figure 1, disks that are displaced into an alley, even by a small amount, become easily visible (McAnany and Levine 2005). We therefore tested the effects of curvature when the disks were displaced by one disk radius along the centerline of a horizontal alley. This placed them halfway outside the intersections. (Subject 4 was tested with disks displaced one disk diameter, so that they were entirely outside the intersection; subject 2 was tested with both displacements. There was no noticeable difference between these conditions.)

Displacing light disks greatly reduced their thresholds relative to disks centered within the intersections, but threshold increased when the alleys were curved. The inverse transformed mean correlations of the contrast thresholds *versus* curvature functions for the four subjects tested are shown in the right side of figure 5B. The inverse transform of the mean transformed correlations from all four subjects tested was 0.93; this difference from zero was significant ($t$ = 3.908, 11 *df*, $p$<0.005).

**4 Discussion**

4.1 *Curvature as an inhibitor of detection*

The results of these experiments suggest that curvature of the alleys makes the detection of some features more difficult. The Hermann grid smudges, the scintillating dark spots, and the disks themselves are harder to detect when the alleys are curved. Even dark disks and disks not centered in the intersections, which do not generally vanish, become more difficult to detect when the alleys are curved. Thus, curvature affects detection, and is not specifically an inhibitor of illusory effects.

4.2 *Origin of the effect*

There is evidence that the illusory effects are generated in part at an early stage of processing (e.g.: lateral inhibition in the retina or lateral geniculate nucleus), and in part at a later stage after the inputs from the two eyes have been integrated. Troscianko (1982) tested a skeletal Hermann grid with binocular presentation such that part of the inducing figures appeared in a different plane than the intersection. He concluded that the smudges were mainly (but not entirely) generated peripherally. On the other hand, Wolfe (1984) presented the intersections as crosses; when they were regularly arranged to form the usual Hermann grid, the subjective magnitude of the effect increased with the number of intersections in the display. However, when the crosses were irregularly arrayed there was no consistent increase in magnitude of the effect with number of intersections. Both of Wolfe's findings implicate more central factors than simple lateral inhibition.

Binocular tests of the scintillating grid also implicated central factors for that illusion. Having the disks appear to be in a different plane than the inducing boxes demonstrated a significant central contribution to the illusion, although some peripheral contribution was also present (Schrauf and Spillmann 2000). Dichoptic presentation of the vanishing disk illusion in which the disks were presented to one eye and the grid to the other indicated that illusion was partly due to central mechanisms and partly to peripheral processing (McAnany and Levine 2005); a second experiment verified the contribution of a central component using a binocular presentation in which the disks appeared in a different plane than the grid. However, knowing that the illusory effects occur at two levels does not elucidate the level of operation of curvature.

Geier et al (2004) suggested that the negation of the Hermann and scintillating grid effects by curving the alleys argues against lateral antagonism as the mechanism responsible for these illusions. They established that the net inhibition would be identical whether the alleys were curved or straight, and so the considerable difference between curved and straight alleys could not be due to a change in net antagonism. While it is true that a difference in inhibition cannot account for the difference in effect between straight and curved alleys, this does not mean that inhibition does not contribute to the basic effects. Since curvature makes features harder to detect, features generated by inhibition (the smudges or scintillating dots) would also be harder to see. Moreover, if curvature makes the disks themselves harder to detect, thus lowering their effective contrast, scintillation might not occur because the disks are effectively at too low a contrast to induce the effect.

Another manipulation that reduces the Hermann effect is rotating the grid 45$^{o}$ to a diagonal orientation (Spillmann and Levine 1971; de Lafuente and Ruiz 2004). Curved alleys also produce a twist from vertical and horizontal at each intersection, although the overall grid orientation is maintained. De Lafuente and Ruiz explain the potency of rotation (a total cancellation of the Hermann effect for one of their subjects) as a manifestation of the oblique effect (Campbell and Kulikowski 1966; Appelle 1972; McMahon and MacLeod 2003), in which subjects are more sensitive to vertical and horizontal orientations than oblique orientations. This, in turn, they relate to the orientation tuning of cortical cells.

There are two aspects of cortical cells that could contribute to the oblique effect. There are more cells tuned near vertical and horizontal orientations than are tuned to oblique orientations, and the orientation tuning is narrower for the vertical and horizontal cells than for cells tuned to oblique orientations (Li et al 2003). To explain why rotated grids are less effective, assume that the edges affect fewer cells than if they were oriented along the cardinal axes, although the disks comprise all orientations; in addition, broader orientation tuning might imply weaker lateral inhibition within those cells. Yet it is hard to see how the relatively small differences observed by Li et al (2003) could account for as dramatic a difference as de Lafuente and Ruiz (2004) reported.

We do not believe that the effect of curvature is simply a manifestation of the oblique effect, for two reasons: First, Geier et al (2004) showed that the Hermann and scintillation effects were also eradicated by "knots," circular bulges in the centers of otherwise straight alleys. These would not affect the angles of the alleys as they exit the intersections. Although we did not test knots on the stimuli described here, it is reasonable to assume the effects are similarly caused.

Second, very slight curvature affects the thresholds. While it is true that small deviations can be significant for the oblique effect (Campbell and Kulikowski 1966; Orban et al 1984), the angles that produced a change in sensitivity were exquisitely small. The tangents to the alleys as they departed the intersections were rarely greater than 14$^o$ from vertical or horizontal for the most extreme curvatures tested, and significant effects could be found with angles less than 3$^o$. Moreover, these tangent angles are an overestimate, as the slope of the sinusoidal function rapidly decreases away from the middle of the intersection. Angles to the peak of the sine (1/4 of the alley length) were typically less than 10$^o$, with effects noticeable at 2$^o$.

On the other hand, curved alleys might engage cells of various orientations, and thereby allow for more interaction than if only a pair of orientations were stimulated. Since the circular disks contain all orientations, this might make curves more effective at blocking visibility.

Schiller and Carvey (2005) presented a detailed account of how the Hermann grid illusion and the effects of manipulations of it (including curvature of the alleys) could be explained specifically as a manifestation of the S1 simple cells of primate striate cortex. S1 cells have elongated receptive fields that respond best to edges of a particular polarity moving in a particular direction (Schiller et al 1976a). Their argument is that intersections interrupt the edges formed by the boxes, and thus reduce the firing of these cells. Curving the alleys also disrupts the edges, and since the edges are disrupted within alleys as well as across intersections, no difference would be produced between alley and intersection. To explain the loss of effect with rotation to $45^{o}$, they invoke the oblique effect and the orientation tuning of S1 cells.

The small curvatures that result in increased thresholds, however, would hardly be sufficient to preclude responses by edge detecting cells. We note that fewer than 10% of S1 cells have orientation tuning finer than $25^{o}$ (Schiller et al 1976b, Fig. 3). Moreover, it is hard to see why reducing the responses of S1 cells would affect the detection of dark disks or disks displaced from the centers of the intersections.

4.3 *Complexity*

We consider that a more likely explanation is that the locally complex nature of the curved alleys engages “higher” mechanisms that concentrate perceptual attention upon the alley features and thereby tend to eclipse the information about the disks. In this sense, the effect of curvature may be a result of the sophistication of the network of processing that leads from sensation to perceptual experience. Alternatively, complexity could be recruiting a high-order inhibitory mechanism such as the lateral prefrontal cortex inhibition of distracters (Tsushima et al 2006).

Complexity is difficult to define. In an intuitive sense, one may say that curved grids are more complex in that they involve more cortical neurons by including more orientations, and perhaps require more processing to make sense of the array of different cells stimulated. (Note that the increase in number of neurons is opposite to the explanation offered by de Lafuente and Ruiz 2004.)

For a more quantitative definition of complexity, one might consider the Fourier power spectra of the various grids. We created images of the eight tetragons in one block of our displays, and found that their total Fourier power increased less than linearly with curvature.

The most direct measure of complexity might be the information content of patterns with various degrees of curvature (Attneave 1954). The estimated information depends on the resolution of the calculations. We determined the information content of our eight tetragon images from all the possible two-by-two pixel tiles in the images, and again from all possible three-by-three, four-by-four, and five-by-five pixel tiles. We compared these results to the efficiency of standard image compression algorithms by converting our eight tetragon images to jpg files (which depend on eight-by-eight, or 64-pixel, tiles) and tif files. The size of the files as a function of curvature should represent a measure of the effective information content of the images. Of course, to compare to our data we must adjust for the arbitrary conversion from bits to contrast, and add a vertical shift to account for the unaffected components.

These methods of deducing complexity all produce similar forms of the relationship between complexity and curvature of the alleys. All the methods produced negatively accelerated (but increasing) curves. The Fourier power and compressed file results did not differ noticeably from each other when they were scaled and shifted to the same vertical axes. The direct calculations of information were more nearly linear, with the deviation from linearity increasing with the size of the sampling tiles used for the calculations. These curves are shown as progressively darker curves in figure 6. For comparison, the mean of the Fourier power, jpg compression, and tif compression is presented as the heavier gray continuous curve in figure 6.

figure 6 near here

Estimates of complexity provide a benchmark for our data. The effect of curvature is graded, but the largest change in many conditions occurs for the smallest curvatures, consistent with the pattern of increase of complexity with curvature. If the pure obscuring function (that is, the effect of curvature on dark disks, for which there is no confounding illusory effect) is compared to complexity, there is good concordance. This is shown by the triangles and dotted lines in figure 6, which are the data for subject 4 detecting dark disks. The data from the other three subjects who were tested with dark disks are similarly close to a scaled and shifted version of the complexity function.

The functions for detection of light disks do not fit the functions for complexity as closely as do the functions for dark disks. To make the comparison, these threshold contrasts are rescaled to account for their much higher thresholds (but not also shifted relative to the dark disk curves because a sensitivity difference should be represented by a simple multiplicative factor). The detection of the vanishing disk by subject 4 is shown in figure 6 by diamonds with dashed lines. Although the function is variable (these are data from a single run), the values for high curvatures are roughly consistent with the complexity functions. The two lowest curvatures, however, present higher thresholds than would be expected. The scaled data for light disks from the other three subjects also fit the complexity curves (scaled to their data for dark disks) for large curvatures, but thresholds are higher than expected for curvatures less than 2%.

An explanation for the discrepancies at low curvature may be found in a spontaneous comment made by subject 4, who noted some confusion at low curvature because the gray Hermann illusion smudges interfered with her ability to judge the presence of light disks near threshold. These smudges would not be present with larger curvatures. The light disks should be rendered increasingly more difficult to detect with increasing complexity just as the dark disks are, but the smudges raise thresholds at the lowest curvatures. The smudges may slightly lower threshold for the dark disks at low curvatures by sub-threshold summation. The dip around 2% curvature in the data from light disks may be an indication that the Hermann smudges are not evident at that curvature, and the threshold is determined purely by complexity; with less curvature, threshold is raised by the smudges. Slight curvature can produce a threshold comparable to that with no curvature because of the opposing effects of curvature: raising disk threshold while reducing the salience of the smudges. We thus conclude that image complexity interferes with the ability to detect features, be they smudges, scintillations, or the disks themselves.

**Footnote for page 8**

* The relationship among step sizes and their effect upon staircase convergence may best be appreciated by an example. Consider a point in the sequence of trials at which all four disks are at the same baseline (perceptual) level, represented as the set {0,0,0,0}. For simplicity, assume the subject always chooses one of the highest level disks (the result is the same if a lower level disk is occasionally selected, but more trials are required to achieve the “final” state). Then, for a decrement of three units and an increment of one, the sequence will be {0, 0, 0, 0} →{-3, 1, 1, 1} →{-2, -2, 2, 2} →{-1, -1, -1, 3} →{0, 0, 0, 0}. There will be no change after four trials. If the decrement were less, say two units, the sequence would be: {0, 0, 0, 0} →{-2, 1, 1, 1} →{-1, -1, 2, 2} →{0, 0, 0, 3} →{1, 1, 1, 1}. The values will inexorably increase. But if the decrement were larger, say four units, then {0, 0, 0, 0} →{-4, 1, 1, 1} →{-3, -3, 2, 2} →{-2, -2, -2, 3} →{-1, -1, -1, -1}. The values will inexorably decrease. We found a decrement of eight to be efficient: {0, 0, 0, 0} →{-8, 1, 1, 1} →{-7, -7, 2, 2} →{-6, -6, -6, 3} →{-5, -5, -5, -5}. Thus, the disks would all grow dimmer were it not for the “nothing visible” option that increases all the luminances.

**References**:

Appelle S, 1972 "Perception and discrimination as a function of stimulus orientation" *Psychological Bulletin* **78** 266-278

Attneave F, 1954 "Some informational aspects of visual perception" *Psychological Review* **61** 183-193

Campbell F W, Kulikowski J J, 1966 "Orientational selectivity of the human visual system" *Journal of Physiology (London)* **187** 437-445

de Lafuente V, Ruiz O, 2004 "The orientation dependence of the Hermann grid illusion" *Experimental Brain Research* **154** 255-260

Ehrenstein W H, Spillmann L, Sarris V, 2003 "Gestalt issues in modern neuroscience" *Axiomathes* **13** 433-458

Geier J, Sera L, Bernath L, 2004 "Stopping the Hermann grid illusion by simple sine distortion" ECVP 2004 abstract

Li B, Peterson M R, Freeman R D, 2003 "Oblique effect: A neural basis in the visual cortex" *Journal of Neurophysiology* **90** 204-217

McAnany J J, Levine M W, 2004 "The blanking phenomenon: a novel form of visual disappearance" *Vision Research* **44** 993-1001

McAnany J J, Levine M W, 2005 "A psychoanatomical investigation of the blanking phenomenon" *Vision Research* **45** 193-203

McMahon M, MacLeod D I A, 2003 "The origin of the oblique effect examined with pattern adaptation and masking" *Journal of Vision* **3** 230-239

Orban G A, Vandenbussche E, Vogels R, 1984 "Human orientation discrimination tested with long stimuli" *Vision Research* **24** 121-128

Schiller P H, Carvey C E, 2005 "The Hermann grid revisited" *Perception* **34** 1375-1397

Schiller P H, Finlay B L, Volman S F, 1976a "Quantitative studies of single-cell properties in monkey striate cortex. I. Spatiotemporal organization of receptive fields" *Journal of Neurophysiology* **39** 1288-1319

Schiller P H, Finlay B L, Volman S F, 1976b "Quantitative studies of single-cell properties in monkey striate cortex. II. Orientation specificity and ocular dominance" *Journal of Neurophysiology* **39** 1320-1333

Schrauf M, Lingelbach B, Wist E R, 1997 "The scintillating grid illusion" *Vision Research* **37** 1033-1038

Schrauf M, Spillmann L, 2000 "The scintillating grid illusion in stereo-depth" *Vision Research* **40** 717-721

Spillmann L, 1994 "The Hermann grid illusion: a tool for studying human perspective field organization" *Perception* **23** 691-708

Spillmann L, Levine J, 1971 "Contrast enhancement in a Hermann grid with variable figure-ground ratio" *Experimental Brain Research* **13** 547-559

Troscianko T, 1982 "A stereoscopic presentation of the Hermann grid" *Vision Research* **22** 485-489

Tsushima Y, Sasaki Y, Watanabe T, 2006 "Greater disruption due to failure of inhibitory control on an ambiguous distractor" *Science* **314** 1786-1788

Wolfe J M, 1984, "Global factors in the Hermann grid illusion" *Perception* **13** 33 – 40

**Figure legends**:

**figure 1** Demonstration of the effects of curvature. Fixate on the cross at the bottom of the left part of the figure, and notice which disks remain visible. Then fixate on the cross at the right and compare the appearances of the disks with the corresponding ones on the left.

**figure 2** The stimulus display. The area between the upper and lower grids (containing only a fixation cross) could be of various heights. This example shows a curvature of 4.4% (near the middle of the range used); at this curvature, the peak of the alley aligns with the center point of the intersection, and a tangent to the alley as it leaves the intersection is at an angle of $14.6^{o}$. A line from the intersection center to the middle of the peak of the alley is at an angle of $10^{o}$. Disks of different luminances are shown in each of the four possible disk locations.

**figure 3** Increases in threshold with amplitude of curvature of the alleys. Thresholds are plotted as a percentage of the maximum contrast available. **A.** Thresholds for scintillation. Subject 1: (triangles and dotted lines) separation between upper and lower blocks was $9.3^o$ (from top of lower block to bottom of upper block); the gray of the alleys was 9.9 cd/$m^2$. Three runs included. Subject 2: (squares and dashed lines) separation between upper and lower blocks was $5.3^o$; gray = 24.1 cd/$m^2$. Four runs included. Subject 3: (circles and dot-dash lines) separation between upper and lower blocks was $4.3^o$; gray = 18.0 cd/$m^2$. Single run. Subject 4: (diamonds and heavy line) separation between upper and lower blocks was $2.1\,^o$; gray = 18.0 cd/$m^2$. Single run. **B**. Thresholds for the vanishing disks. Parameters and numbers of runs identical to those for scintillation except subject 3 had three runs, and for subject 4 the separation was $4.3^o$ and there were three runs.

**figure 4** Correlations between threshold contrast and curvature for each subject and for the combined data from all subjects (solid black bars). Left set of bars for detection of scintillation; right large set for detection of the disks. The two smaller graphs to the right represent detection of the disks with four interlaced staircases (upper graph) and with two interlaced staircases (upper and lower fields, lower graph). Values are the inverse Fisher transform of the mean Fisher transforms of the individual correlations. Error bars represent 95% confidence.

**figure 5** Effect of curvature upon visibility of disks not normally obscured by a grid. **A**. Mean absolute value of contrast at threshold relative to maximum available for disks darker than the gray of the alleys. Conventions and symbols as in figure 3A. For subject 1, the separation between upper and lower blocks was 6.3$^{o}$; the gray of alleys was 18.0 cd/m$^2$ (note that there was an additional point at 9.8%); subject 2, separation = 10.5$^{o}$; gray = 24.1 cd/m$^2$; subject 3, separation = 12.6$^{o}$; gray = 18.0 cd/m$^2$; subject 4, separation = 8.4$^{o}$; gray = 18.0 cd/m$^2$. **B**. Correlations for each subject and all subjects combined. Data for dark disks on the left; disks displaced from the centers of intersections shown on the right. Method and conventions as in figure 4.

**figure 6** Comparison of measures of complexity with results from detection of the vanishing disk (solid diamonds and dashed lines) and dark disks (open triangles and dotted lines). Data from Subject 4. Information derived from 2X2 pixel analyses are shown by a thin gray curve; information analyses of 3X3 pixels, 4X4 pixels, and 5X5 pixels are represented by progressively heavier black curves. The mean of Fourier power, jpg compression, and tif compression are shown as a thick gray curve. Estimates of complexity have been scaled and shifted to fit the data from dark disks (least squares criterion). The white disk data are arbitrarily scaled (but not shifted) to correspond with those of the dark disks.

**Figure 1**

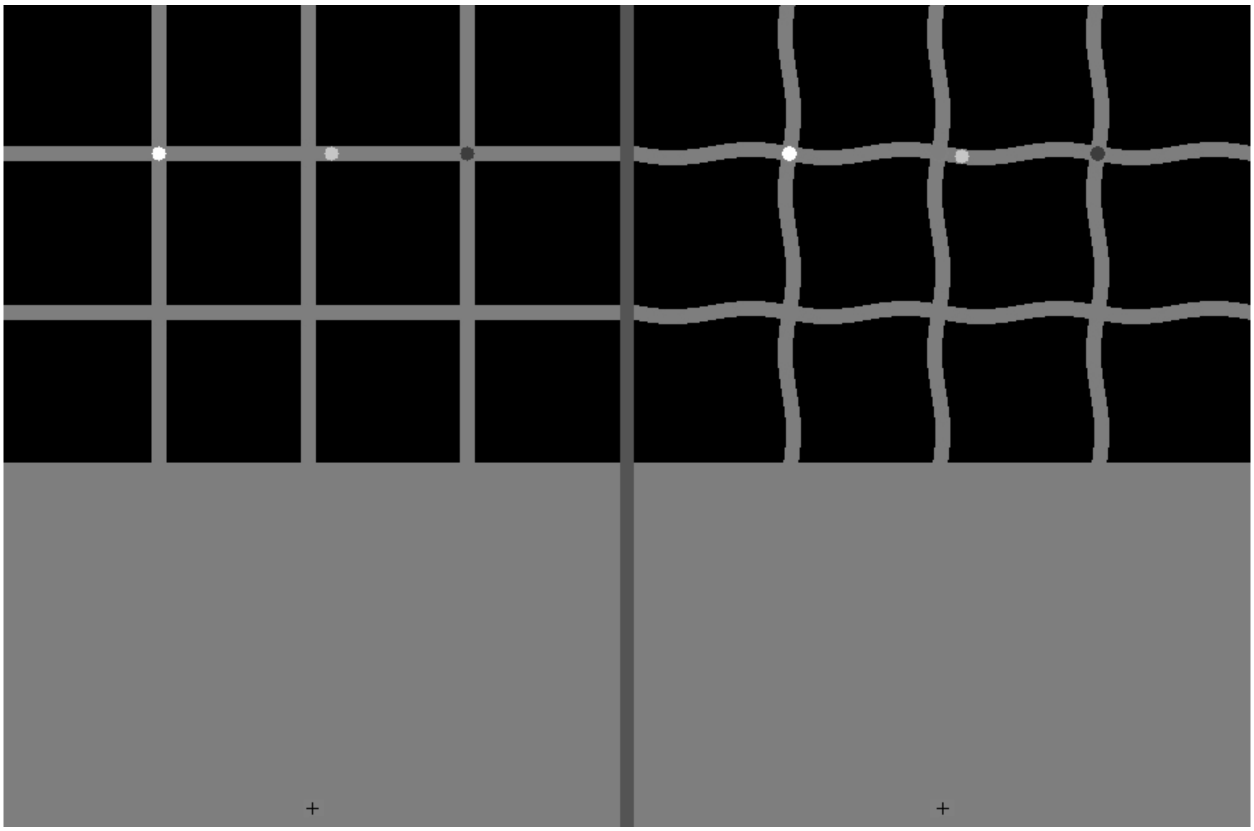

# Figure 2

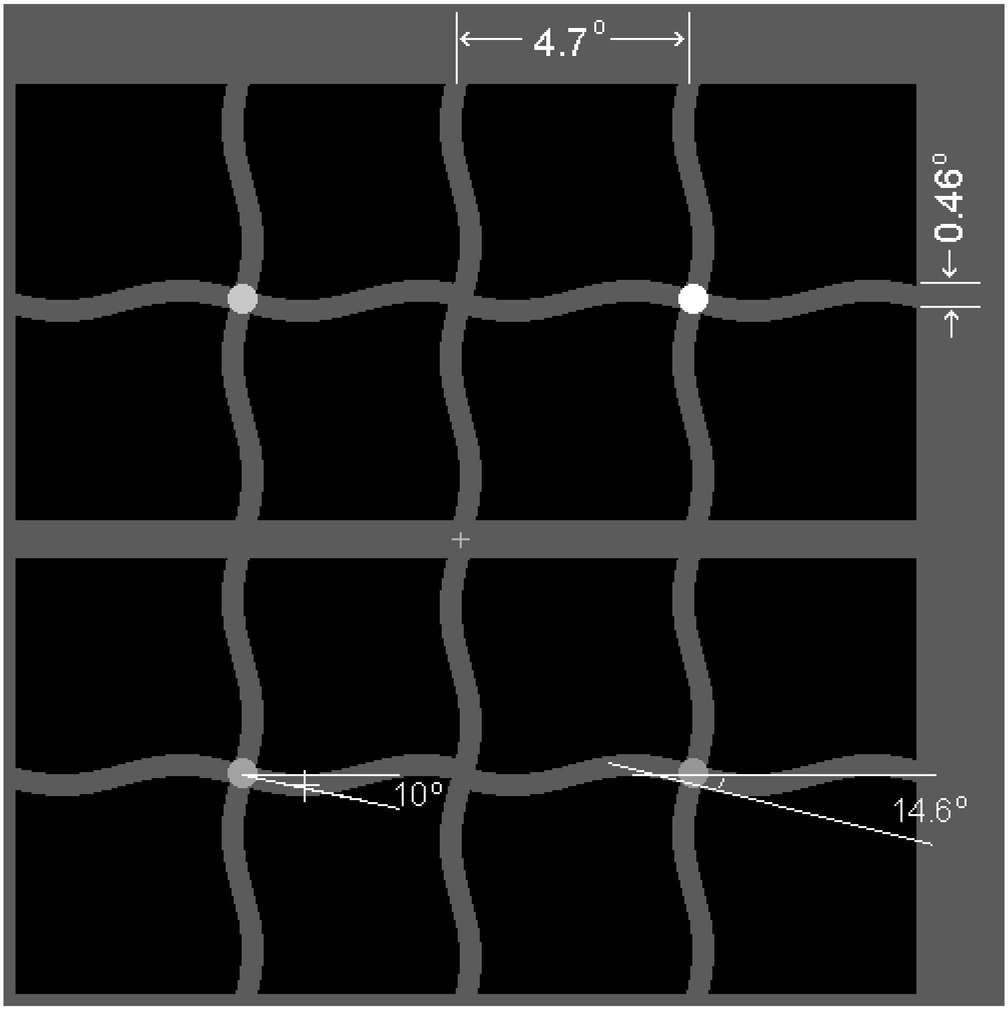

**Figure 3**

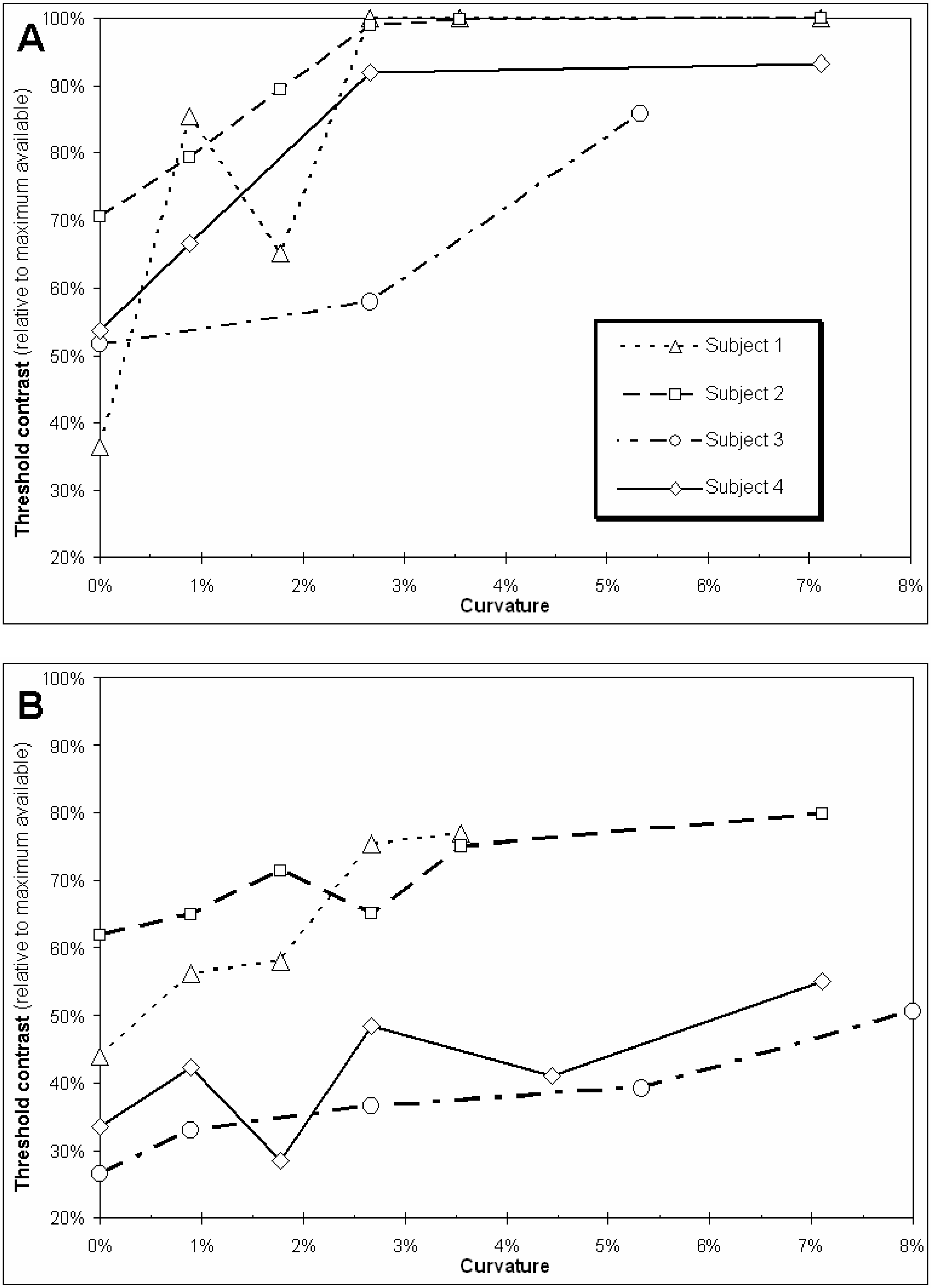
A
B
Threshold contrast (relative to maximum available)
100%
90%
80%
70%
60%
50%
40%
30%
20%
0%
1%
2%
3%
4%
5%
6%
7%
8%
Curvature
Subject 1
Subject 2
Subject 3
Subject 4

**Figure 4**

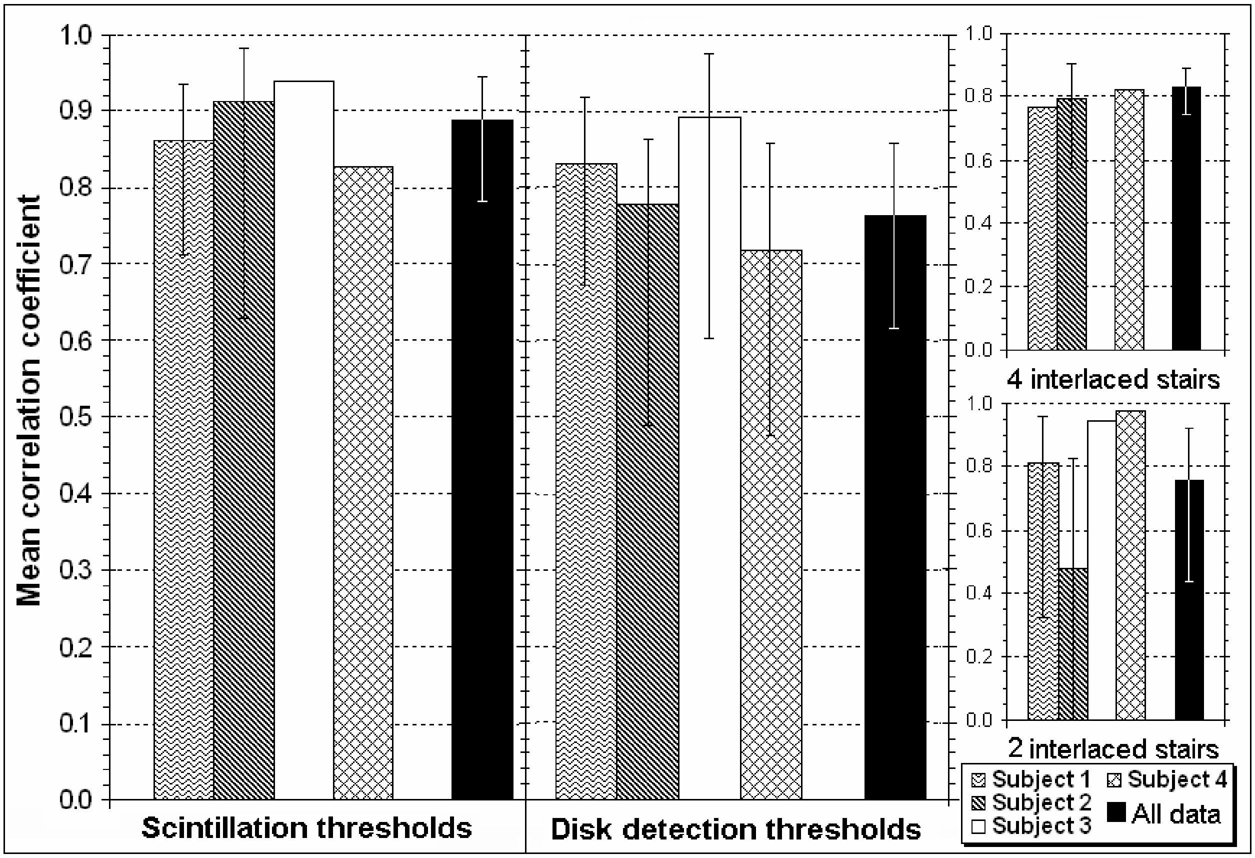
1.0
0.9
0.8
0.7
0.6
0.5
0.4
0.3
0.2
0.1
0.0
Mean correlation coefficient
Scintillation thresholds
Disk detection thresholds
4 interlaced stairs
2 interlaced stairs
Subject 1
Subject 2
Subject 3
Subject 4
All data

**Figure 5**

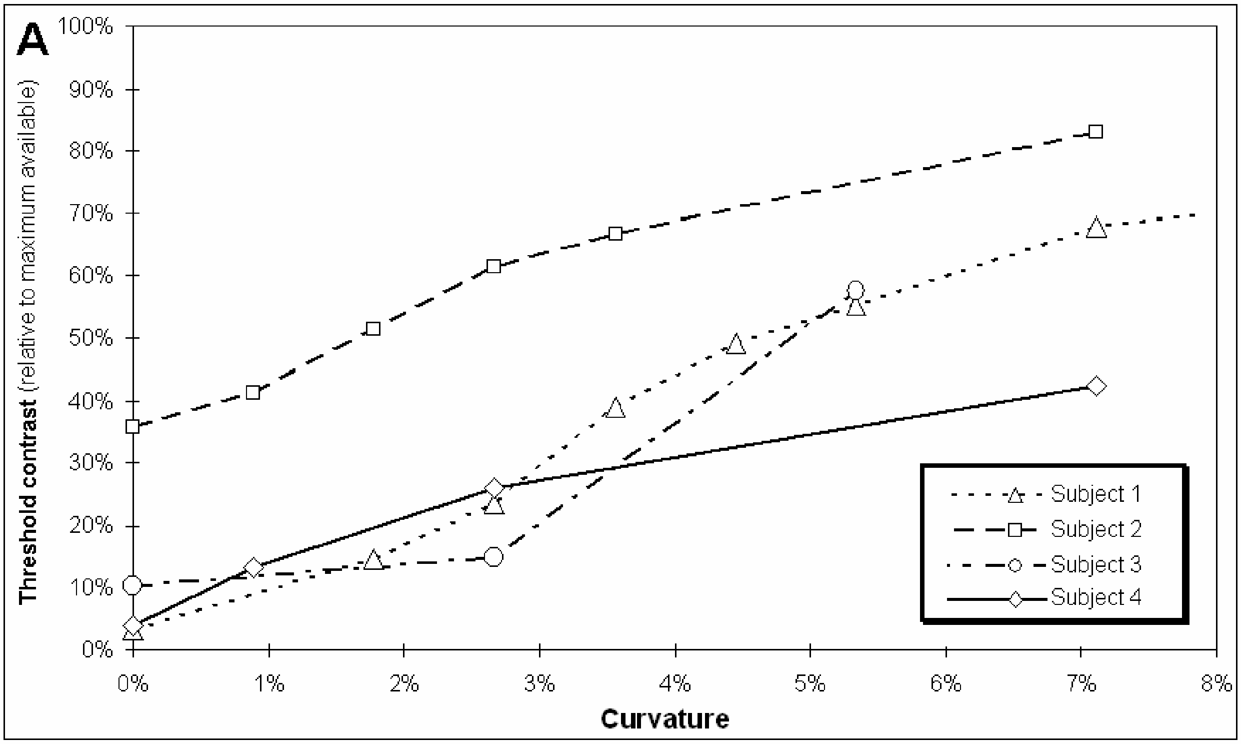
A
Threshold contrast (relative to maximum available)
100%
90%
80%
70%
60%
50%
40%
30%
20%
10%
0%
0%
1%
2%
3%
4%
5%
6%
7%
8%
Curvature
Subject 1
Subject 2
Subject 3
Subject 4

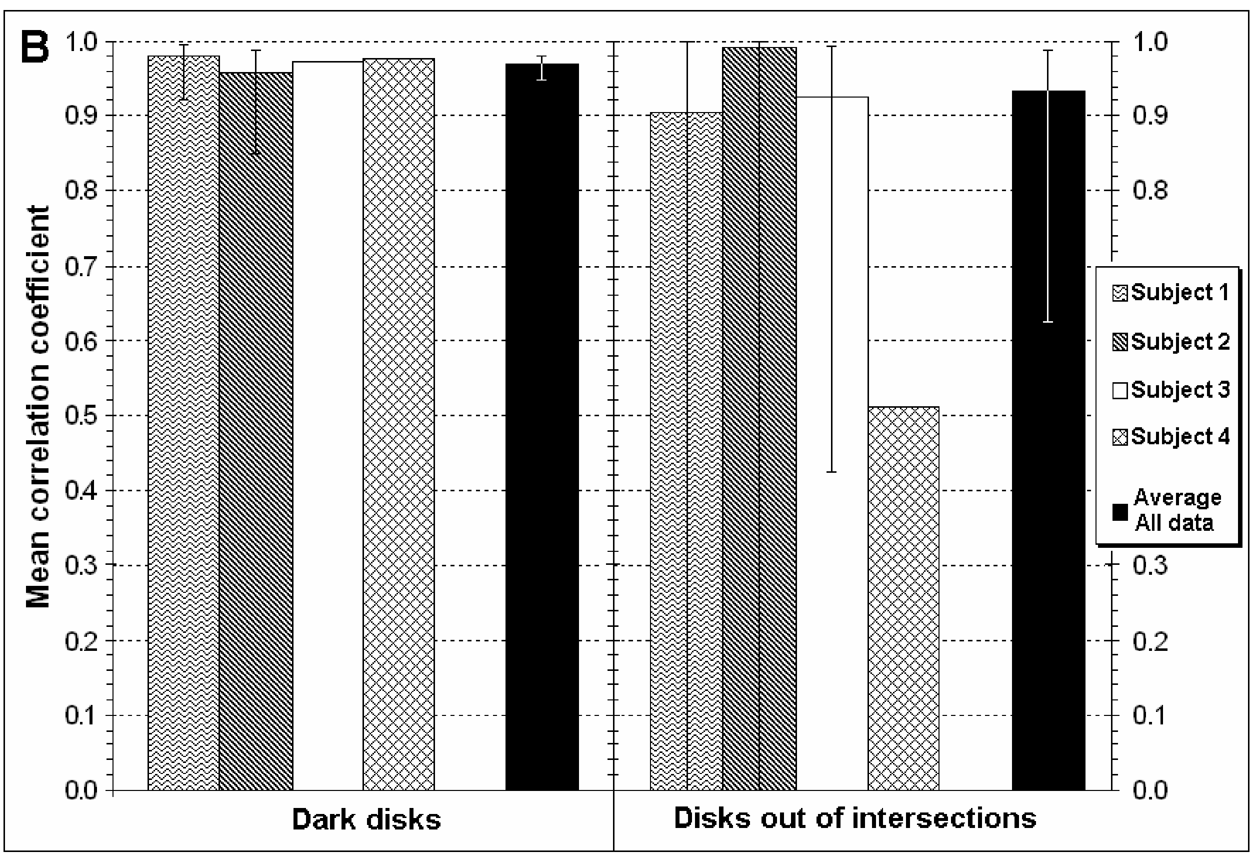
B
Mean correlation coefficient
1.0
0.9
0.8
0.7
0.6
0.5
0.4
0.3
0.2
0.1
0.0
Subject 1
Subject 2
Subject 3
Subject 4
Average All data
Dark disks
Disks out of intersections

**Figure 6**

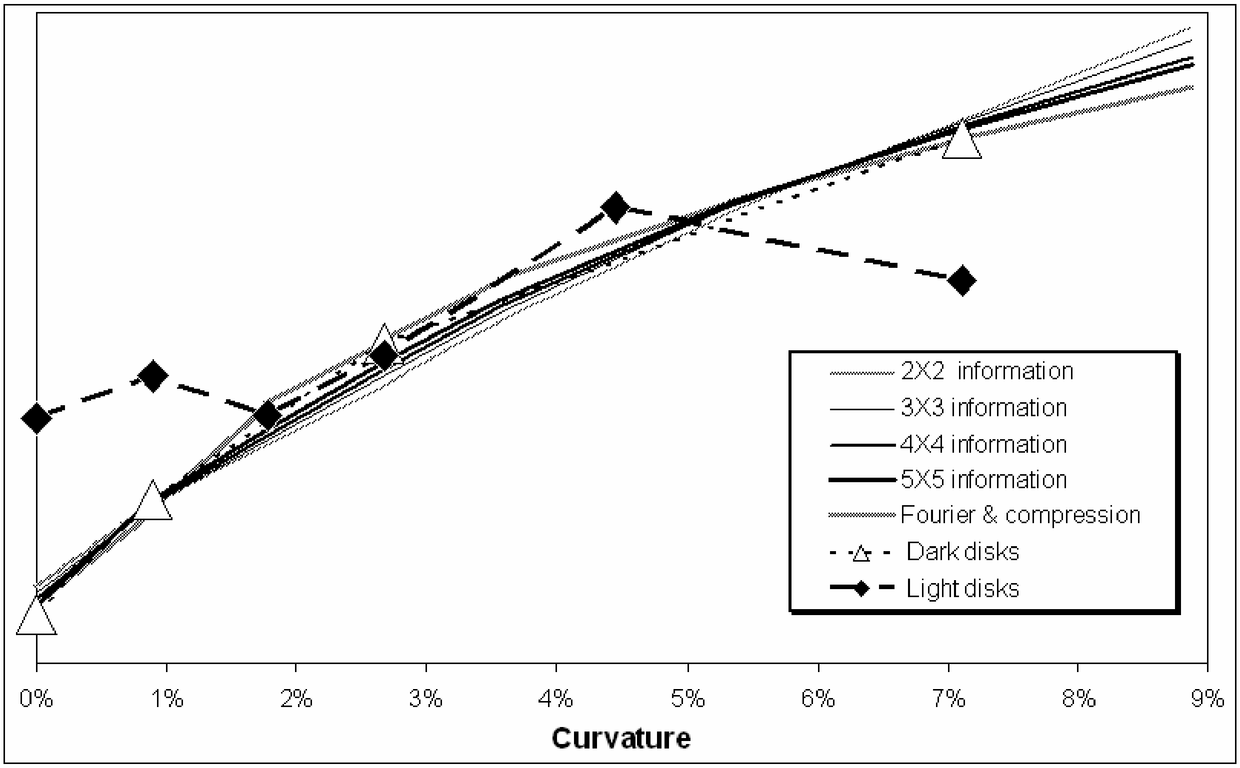
2X2 information
3X3 information
4X4 information
5X5 information
Fourier & compression
Dark disks
Light disks
0%
1%
2%
3%
4%
5%
6%
7%
8%
9%
Curvature